

## Observing Dirac's Classical Phase Space Analog to the Quantum State

Charles Bamber<sup>1,\*</sup> and Jeff S. Lundeen<sup>2,†</sup>

<sup>1</sup>*Measurement Science and Standards, National Research Council, Ottawa, Canada K1A 0R6*

<sup>2</sup>*Physics Department, University of Ottawa, 150 Louis Pasteur, Ottawa, Canada K1N 6N5*

(Received 5 September 2013; revised manuscript received 29 November 2013; published 19 February 2014)

In 1945, Dirac attempted to develop a “formal probability” distribution to describe quantum operators in terms of two noncommuting variables, such as position  $x$  and momentum  $p$  [Rev. Mod. Phys. **17**, 195 (1945)]. The resulting quasiprobability distribution is a complete representation of the quantum state and can be observed directly in experiments. We measure Dirac's distribution for the quantum state of the transverse degree of freedom of a photon by weakly measuring transverse  $x$  so as to not randomize the subsequent  $p$  measurement. Furthermore, we show that the distribution has the classical-like feature that it transforms (e.g., propagates) according to Bayes' law.

DOI: 10.1103/PhysRevLett.112.070405

PACS numbers: 03.65.Ta, 03.65.Wj, 03.67.-a, 42.50.Dv

When formulating quantum theory, many physicists sought a classical interpretation of the object at its center, the quantum state. The most well-known of these is the Wigner function  $W(x, p)$ , an attempt to produce a joint probability distribution for a particle's instantaneous momentum and position [1]. These “phase-space” distributions necessarily violate many of the properties that classical probability distributions must obey. However, they are useful for visualizing concurrent momentum and position features in quantum states, which might be obscurely encoded in the phase of the wave function or the off-diagonal elements of the density matrix. Additionally, a nonclassical hallmark in the distribution (e.g., negative probabilities) can be used to identify intrinsically quantum states [2]. It is remarkable that even though the quantum state has been an overwhelmingly successful concept and tool for almost a century, our understanding of its nature is still being refined [3]. These distributions have contributed to this refinement [4] and have helped demarcate the boundary between classical and quantum phenomena [5].

In quantum physics, Heisenberg's uncertainty relation implies that a precise joint measurement of position  $X$  and momentum  $P$  is impossible. Contrast this with classical physics, in which a particle has a definite and unique position  $x$  and momentum  $p$  at any moment in time, thereby defining its “state.” Measuring a classical particle's state then just entails a joint measurement of  $X$  and  $P$ . Equivalently, one can measure whether a particle is at a particular point  $(x, p)$  in “phase space” (i.e.,  $X$ - $P$  space) and then raster over  $x$  and  $p$ . And, if the particle is produced in a random process such that it is in a random distribution of states, then repeated measurements at each point will let us find the average result: the probability for the particle to be at that point  $\mathbb{P}(x, p)$ , a phase-space probability distribution.

Consider what the quantum version of this measurement would be by beginning with the classical description of this phase-space point, a two-dimensional (2-d) Dirac delta function centered at  $x$  and  $p$ ,  $\delta^{(2)}(X - x, P - p)$ . Crucially,

there is no unique nor general method for translating a classical observable to its quantum equivalent [6]. For example, since they do not commute, one must choose an ordering  $O$  of quantum operators  $\mathbf{X}$  and  $\mathbf{P}$  with which to replace classical variables  $X$  and  $P$ ,  $\Delta_O(x, p) = \{\delta^{(2)}(\mathbf{X} - x, \mathbf{P} - p)\}_O$ . In this Letter, we experimentally demonstrate the measurement of this operator for the antistandard ordering (i.e.,  $\mathbf{P}$  is always to the left of  $\mathbf{X}$ ),  $\Delta_{AS}(x, p) = \delta(\mathbf{P} - p)\delta(\mathbf{X} - x) = \boldsymbol{\pi}_p \boldsymbol{\pi}_x$ , where  $\boldsymbol{\pi}_m = |m\rangle\langle m|$  is a projector. Numerous other orderings are possible, and each corresponds to a distinct point operator  $\Delta_O$ , which may or may not describe a physical measurement (an “observable”). The average result of such a measurement then would be the quantum version of our classical state measurement procedure outlined above.

As usual, this average result is equal to the expectation value of the operator,  $\langle \Delta_O(x, p) \rangle = \text{Tr}[\Delta_O(x, p)\rho]$ , where  $\rho$  is the density operator describing the quantum state of the particle. It may come as a surprise that this simple, classically motivated measurement procedure will completely determine the quantum state. Whereas classically it gives the probability  $\mathbb{P}(x, p)$ , the quantum version gives a “quasiprobability”  $\mathbb{P}_{\bar{O}}(x, p) = \langle \Delta_{\bar{O}} \rangle$  [7,8], where  $\bar{O}$  is the reverse ordering to  $O$ . That is, for typical orderings  $O$ , the average result is a phase-space quasiprobability distribution in  $x$  and  $p$  equivalent to the state of the particle.

From this perspective, the Wigner function corresponds to a direct measurement of an  $(x, p)$  point observable that has been symmetrically ordered (i.e., the “Weyl” ordering  $W$ , with  $W = \bar{W}$ ):  $\Delta_W = \mathbf{R}_\pi(x, p)/\pi$  [9], where  $\mathbf{R}_\pi$  is the parity of a particle about point  $(x, p)$ . The normal  $N$  ordering ( $\mathbf{a}^\dagger$  to the left of  $\mathbf{a}$ , where  $\mathbf{a}$  is the usual lowering operator  $\mathbf{a} = \mathbf{X} + i\mathbf{P}$ ) and its reverse, antinormal  $AN$ , correspond to the other two well-known quasiprobability distributions, the Husimi  $Q$  function [10] [ $\mathbb{P}_N$ ,  $\Delta_{AN}(\alpha = x + ip) = |\alpha\rangle\langle\alpha|/\pi$ , i.e., a projection onto a coherent state  $|\alpha\rangle$  [7]] and the Glauber-Sudarshan  $P$  distribution [11] ( $\mathbb{P}_{AN}$ ,  $\Delta_N$  is unphysical). The Wigner and  $Q$  functions have been directly

measured in various physical systems [12], including the transverse state of a photon [13].

In 1945, Dirac wrote “On the analogy between classical and quantum mechanics,” [14] in which he introduced what we call the “Dirac distribution” as a classical-like representation of a quantum operator, such as the density operator  $\rho$ . Over the past 90 years, this distribution has been repeatedly rediscovered [15,16]. It has since been realized that the Dirac distribution is  $\tilde{\mathbb{P}}_S(x, p)$ , the standard ordered quasiprobability distribution and its complex conjugate is  $\mathbb{P}_{AS}(x, p)$  [7,17,18]. Despite being the product of one of the founders of quantum theory, there has been little experimental investigation of the Dirac distribution. The impediment has been that  $\Delta_{AS} = \pi_p \pi_x$  is non-Hermitian and thus should not be an observable. Physically, this is enforced by the fact that a measurement of  $\pi_x = \delta(\mathbf{X} - x)$  will disturb and, hence, invalidate the subsequent measurement of  $\pi_p = \delta(\mathbf{P} - p)$ , making a joint measurement impossible.

Measurement-induced disturbance can be minimized in quantum physics by: (1) lowering the precision,  $\delta(x) \rightarrow \Delta x$ , and (2) decreasing the certainty of the measurement,  $\text{Prob}(x_{\text{system}}|x_{\text{measured}}) \ll 1$ . An example of the second approach is *weak* measurement: by reducing the coupling between the system and the measurement apparatus, the result from any one trial becomes uncertain [19]. Reducing the coupling similarly reduces the disturbance (i.e., backaction). Moreover, by averaging over many trials, an *average* result can still be found to arbitrarily low uncertainty. Remarkably, the Dirac distribution can be measured simply by replacing the first measurement by a weak measurement [20] of  $\pi_x$ , as we showed in Ref. [21] (see also the related work [22]). We termed the average joint result of this weak-strong position-momentum measurement the “weak average.” In the zero-coupling limit, it is [21]

$$\langle \pi_p^s \pi_x^w \rangle_\rho = \text{Tr}[\pi_p \pi_x \rho] = \langle \Delta_{AS}(x, p) \rangle = \tilde{\mathbb{P}}_S(x, p), \quad (1)$$

where  $\tilde{\mathbb{P}}_S$  is the Dirac distribution (see Supplemental Material [23]). The superscripts *s* and *w* denote strong (i.e., normal) and weak measurements, respectively. (From here on, we omit the *S* subscript as we will deal exclusively with the Dirac distribution.) As an expectation value of a non-Hermitian operator, the weak average is complex in general [24] (the meaning of this will later be explained using our specific experiment as an example). It follows that, unlike the Wigner function and other aforementioned quasiprobabilities, the Dirac distribution is complex.

The Dirac distribution  $\tilde{\mathbb{P}}(x, p)$  possesses the key feature that it can be manipulated according to Bayes’ theorem despite the fact that it is not a true probability [25,26]. For example, we could calculate the conditional quasiprobability of  $x$  given  $p$ :  $\tilde{\mathbb{P}}(x|p) = \tilde{\mathbb{P}}(x, p)/\tilde{\mathbb{P}}(p)$ , where  $\tilde{\mathbb{P}}(p) \equiv \langle \pi_p^w \rangle_\rho = \mathbb{P}(p)$  is defined in analogy to the weak average. One could also directly *measure*  $\tilde{\mathbb{P}}(x|p)$  by

following our naive procedure above but only keeping the results for  $X$  in those cases where  $P = p$ . For  $p = 0$ , this is a succinct description of our previously introduced procedure to directly measure the quantum wave function  $\Psi(x)$  [27]. In this light, one would write  $\Psi(x) \propto \tilde{\mathbb{P}}(x|p=0)$ , which provides wave function with a pithy description: It is the quasiprobability of  $x$  given that  $p$  was found to be zero.

Unlike our wave function measurement procedure [27], the measurement of  $\tilde{\mathbb{P}}(x, p)$  can also determine the state of a system that is “mixed.” i.e., one with classical noise or that is entangled with other systems. In this case, the state is described by a density operator  $\rho$  rather than a wave function  $\Psi(x)$  (i.e., a “pure” state).

As an example, we measure the Dirac distribution of the quantum state corresponding to the transverse position of a photon for mixed and pure states. We clarify what we mean by the photon’s quantum state in the Supplemental Material [23]. Recent work has measured the Dirac distribution in a discrete system [28] but only for the pure case, and only in a simple two-level system. Shown in Fig. 1, our experimental setup builds on the one in Ref. [27]. Our photons are produced by an attenuated laser (wavelength = 780 nm) and coupled into a single-mode fiber. Although we do not use single-photon states, one can say that every photon that exits the fiber output will have the same transverse state; they form an identical ensemble of particles. The photons are linearly polarized and collimated by a convex lens (achromat, focal length  $f = 30$  cm, diameter  $d = 5$  mm) and sent through an aperture ( $x \times y$  dimensions =  $44 \text{ mm} \times 2 \text{ mm}$ ). Unlike in Ref. [27], just before the lens, we introduce phase noise by rotating a 4 mm thick glass plate by 4 deg about a horizontal rotation axis at 11 Hz, thereby generating many waves of phase delay. The plate extends

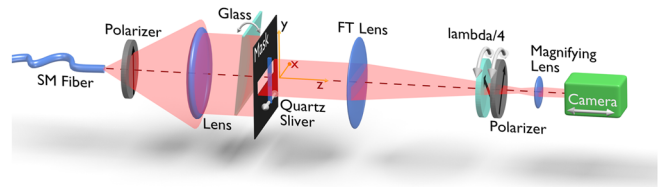


FIG. 1 (color online). Experimental setup to directly measure the Dirac quasiprobability distribution  $\tilde{\mathbb{P}}(x, p)$  of the transverse state of a photon. Photons emerge from a single-mode fiber and are collimated to produce an identical ensemble in an initial pure state. This is optionally transformed to a mixed state by noise introduced by an oscillating glass plate. A weak measurement of transverse position  $\pi_x = |x\rangle\langle x|$  is implemented by a small polarization rotation  $\varphi = 12.92^\circ$  created by a quartz sliver at  $x$ . This weak measurement is read out jointly with the transverse momentum  $p$  by using a camera, polarizer, and quarter-wave plate in the Fourier transform plane to measure  $\langle \pi_p \sigma^- \rangle = \tilde{\mathbb{P}}(x, p) \sin\varphi$ . We repeat this measurement after displacing the camera from the Fourier transform plane by  $\Delta z$  in order to investigate how the distribution propagates in space.

only over one half of the transverse state. With the glass stationary, the transverse state's phase is discontinuous at the position of the plate edge. With it oscillating, the two halves of the state are completely incoherent over the time scale of our measurements and, thus, the state is mixed.

We divide the weak measurement of  $\pi_x = |x\rangle\langle x|$  into two stages: coupling and readout. The coupling stage occurs just after the collimating lens. This is the plane in space at which we measure the Dirac distribution of the photon ensemble. Here, a quartz sliver (width  $\Delta x = 1$  mm) rotates the photon polarization (initially  $0^\circ$ ) to  $\varphi$  deg at position  $x$ . For  $\varphi = 90^\circ$  this would be a strong measurement, whereas by setting  $\varphi \ll 90^\circ$  our measurement becomes weak. The sliver is also slightly tilted about the  $x$  axis in order to null any phase shift it induces. As described in Ref. [27], we can read out by measuring  $\langle \pi_x^w \rangle = (\langle s | \sigma_x | s \rangle - i \langle s | \sigma_y | s \rangle) / \sin \varphi = \langle s | \sigma^- | s \rangle / \sin \varphi$ , where  $|s\rangle$  is the polarization state of the photon,  $\sigma_x$  and  $\sigma_y$  are the Pauli operators, and  $\sigma^- = \sigma_x + i\sigma_y$  is the lowering operator [29]. The real part and imaginary parts of the weak value are proportional to the shift from zero of the average value of  $\sigma_x$  and  $\sigma_y$ , respectively. Thus, as expected the two parts separately appear in conjugate variables of our measurement apparatus, that is, in the linear and circular polarizations.

In order to perform a *joint* measurement of  $\pi_p \pi_x$ , we must make polarization measurements at each momentum. To do so, a lens (achromat,  $f_{FT} = 1$  m,  $d = 5$  cm) is placed one focal length after the sliver. The Fourier transform (FT) of the quantum state forms in the plane one focal length past the lens. Consequently, the transverse position  $x_{FT}$  in this FT plane is proportional to the transverse momentum  $p$  of the photon at the sliver. We magnify ( $M = 4.935$ ) by another lens ( $f = 35$  mm,  $d = 2.5$  cm) so that the final scaling is  $p = x_{FT} h / (f_{FT} M \lambda)$ , where  $h$  is Planck's constant. To read out  $\langle \pi_x^w \rangle$  we project onto a circular or linear polarization by inserting a quarter-wave plate ( $\lambda/4$ ) and/or polarizer (Pol, Nanoparticle Linear Film Polarizer, Thorlabs LPVIS50) just before the magnifying lens. Then, position and momentum are jointly measured by measuring  $\pi_p \sigma^-$ . We do so by recording the average number of photons  $N_{p,j}$  arriving at each transverse position  $x_{FT}$  on a camera sensor (Basler acA 1300–30  $\mu\text{m}$ , pixel size:  $3.75 \mu\text{m} \times 3.75 \mu\text{m}$ ,  $x \times y$  array size:  $1296 \times 966$ , 12 bit) for two pairs of polarization measurements:  $j = 45^\circ$  and  $-45^\circ$  polarizations and right- ( $\odot$ ) and left-hand ( $\ominus$ ) circular polarizations. For  $\varphi \ll 90^\circ$ , the differences in each pair are proportional to the real and imaginary parts of the Dirac distribution,

$$\tilde{\mathbb{P}}(x, p) \sin \varphi = \frac{N_{p,45^\circ} - N_{p,-45^\circ}}{N_{p,45^\circ} + N_{p,-45^\circ}} - i \frac{N_{p,\odot} - N_{p,\ominus}}{N_{p,\odot} + N_{p,\ominus}}, \quad (2)$$

which is just  $\langle \pi_p \sigma^- \rangle$ . Each polarization measurement is a 1.8 s camera exposure in which we average along the  $y$

dimension to arrive at a vector  $N_{p,j}$ . We take the mean of the weak average over 10 scans of  $x$ .

We directly measure the Dirac distribution  $\tilde{\mathbb{P}}(x, p)$  for the transverse quantum state by measuring these polarization differences for every  $p$  as a function of the sliver position  $x$ , which we move in steps of 1 mm across the aperture of the collimating lens. The insets of Fig. 2 plot this pair of polarization differences as the real and imaginary parts of  $\tilde{\mathbb{P}}(x, p)$  according to Eq. (2). Figures 2(a) and 2(b) display the measured Dirac distribution for the case where the glass plate is stationary (pure state) and oscillating (mixed state), respectively. As can be seen in the phase plots (lower plots), there is a state-independent phase of  $\exp(-ixk)$ , inherent to the Dirac distribution, imposed on the underlying 2-d form of the state in (a) and (b). This overlay phase structure allows one to immediately see phase jumps, such as the one in the pure state (a) at  $x = 25$  mm (the glass edge). In contrast, in the mixed state (b), the phase fringes on either side of  $x = 25$  mm are unrelated, a signature of the lack of phase coherence across this point. Looking now at the magnitude (upper plots), both the mixed and pure states exhibit a depression at  $x = 25$  mm, likely due to photons being scattered out of the apparatus by the glass edge. In the momentum direction, the width of the mixed state is broader than that of the pure state, as expected due to the reduced spatial coherence of the former. This is accompanied by a decreased magnitude since the distribution is normalized to one. These distinctive features suggest that the Dirac distribution provides a useful way to visualize key characteristics of pure and mixed quantum states.

The Dirac distribution is related in a simple way to the position density matrix of the state,  $\rho(x, x') = \langle x | \rho | x' \rangle = \text{FT}[\tilde{\mathbb{P}}(x, p) \exp(ipx/h)](x')$ , where the Fourier

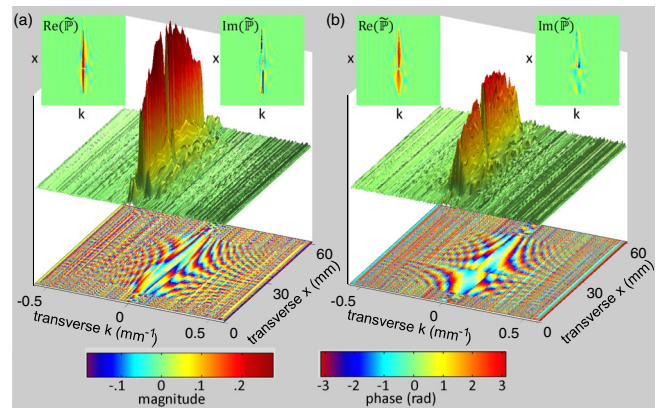


FIG. 2 (color online). Directly measured Dirac distributions for (a) pure and (b) mixed states. In both (a) and (b), the left and right insets are the directly measured real and imaginary parts of the Dirac distribution  $\tilde{\mathbb{P}}(x, p)$ . From these, we calculate the magnitude (upper plot) and phase (lower plot) of the distribution. Transverse  $x$  corresponds to the position of the quartz sliver (i.e.,  $|x\rangle\langle x|$ ); transverse  $k = p/h$  is the transverse wave vector.

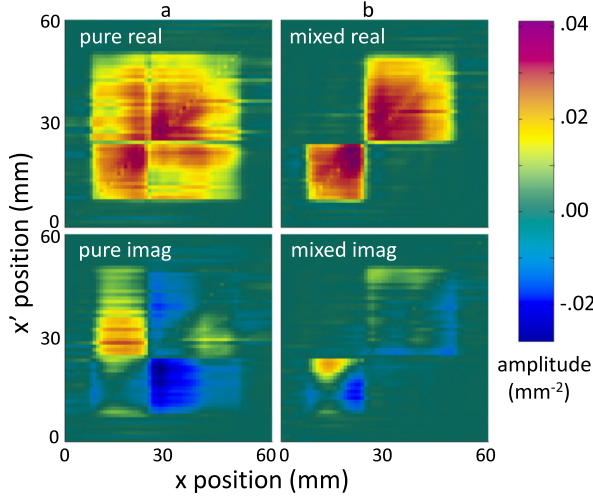


FIG. 3 (color online). Density matrices  $\rho$  for (left plots) pure and (right plots) mixed states, calculated from data presented in Fig. 2. The upper plots and lower plots correspond to the real and imaginary parts of  $\rho$ , respectively. Since we are not in the limit of a zero interaction-strength measurement ( $\varphi = 0$ ), there will still be some backaction due to the measurement. While in the Dirac distribution this leads to minor offsets  $\tilde{\mathbb{P}}(x, p) \rightarrow \tilde{\mathbb{P}}(x, p) - \text{Prob}(x)(1 - \cos(\varphi))$  everywhere, in the density matrix it leads solely to a suppression, by  $\cos(\varphi)$ , of the diagonals, which we correct for in this Figure (see the Supplemental Material for details [23]).

transform FT is performed with respect to momentum  $p$  [18]. In Fig. 3, we plot the position density matrix for each of the Dirac distributions from Fig. 2. For the pure state of Fig. 3(a), the hard edges of the aperture form a square outline in  $\rho$  and the phase jump now appears at both  $x = 25$  mm and  $x' = 25$  mm. Strikingly, in the mixed state in Fig. 3(b) the off-diagonal regions for  $x \leq 25$  mm,  $x' > 25$  mm, and the reverse are close to zero. This is indicative of the lack of coherence between the part of the state that passes through the oscillating glass and the part

that does not. This shows that we can successfully measure the Dirac distribution for a transverse quantum state and that it correctly determines the state of a mixed system.

The compatibility of Bayes' theorem with the Dirac quasiprobability distribution goes beyond the simple example we gave earlier. The simplicity of Dirac distribution allows us to generalize its theoretical definition to multiple variables, e.g.,  $\mathbb{P}(x, q', k', p) = \langle \delta(\mathbf{P} - p)\delta(\mathbf{K}' - k')\delta(\mathbf{Q}' - q')\delta(\mathbf{X} - x) \rangle = \text{Tr}[\pi_p \pi_{k'} \pi_{q'} \pi_x \rho]$ , where  $Q'$  and  $K'$  are another two continuous variables (e.g., the photon position and momentum at a later time after undergoing some evolution). Hoffman showed that with the above theoretical definition of  $\tilde{\mathbb{P}}(x, q', k', p)$  one can propagate the Dirac distribution  $\tilde{\mathbb{P}}(x, k)$  in time by applying Bayes' theorem [26]:

$$\tilde{\mathbb{P}}(q', k') = \sum_{x, p} \tilde{\mathbb{P}}(q', k'|x, p) \cdot \tilde{\mathbb{P}}(x, p), \quad (3)$$

where  $\tilde{\mathbb{P}}(q', k'|x, p) = \tilde{\mathbb{P}}(x, q', k', p)/\tilde{\mathbb{P}}(x, p) = \langle p|k' \rangle \times \langle k'|q' \rangle \langle q'|x \rangle / \langle p|x \rangle$  is independent of the quantum state. This four-dimensional generally complex conditional quasiprobability is a propagator of an arbitrary point in  $x, p$  phase space to any point in  $q', k'$  phase space. In the context of quantum information, it functions like a superoperator (i.e., it transforms between density operators) and can encompass both the unitary and nonunitary evolution of any quantum process (see Ref. [30] for further development of this concept). Note that this is very different from using Bayes' theorem to update a prior quantum state based on the incomplete information about the system provided by classical positive-valued statistics, e.g., POVMs (as studied in Ref. [31]). In particular, here, as with classical probability distributions, one can directly apply Bayes' theorem to update the Dirac quasiprobability distribution and evolve it as a function of space or time.

We now describe a demonstration of this Bayesian propagation. For the sake of experimental simplicity, we

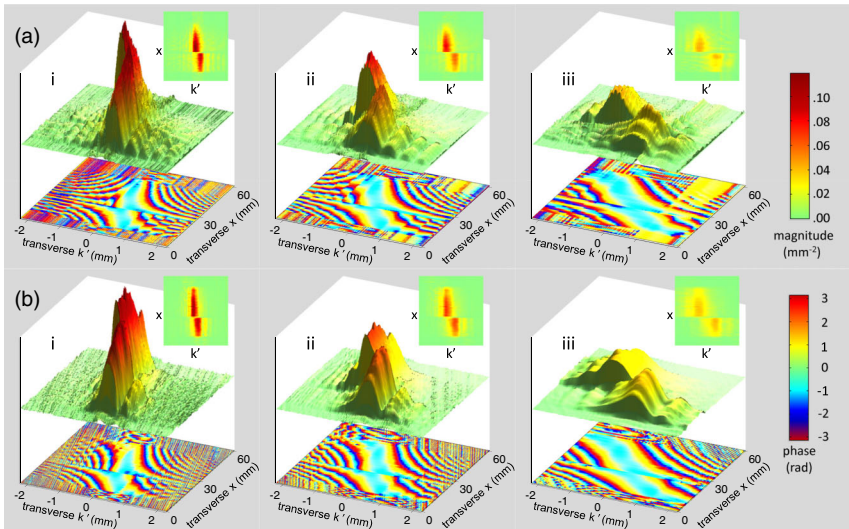


FIG. 4 (color online). Evolution of the quantum state by Bayes' theorem. (a) A series of directly measured Dirac distributions propagated from the mixed state in Fig. 2(b) to a plane translated by  $\Delta z =$  (i) 8.4 cm, (ii) 16 cm, and (iii) 32.5 cm past the Fourier transform plane (by moving the camera). (b) The theoretical prediction for the propagated distributions found using Bayes' theorem, as in Eq. (3). In all (a) and (b) and (i)–(iii), the bottom plot is Dirac distribution's phase and both the inset and top plot are its magnitude. As in Fig. 2, the transverse  $x$  axis is the position of the weak measurement, whereas transverse  $k'$  now corresponds to the transverse position on the camera (which is no longer proportional to momentum).

only update one of the variables in the Dirac distribution  $\tilde{\mathbb{P}}(x, p)$  to arrive at  $\tilde{\mathbb{P}}(x, k') = \langle \pi_{k'}^s \pi_x^w \rangle_\rho$ . By moving the camera back from the reimaged Fourier transform plane so that the photons travel a further distance  $\Delta z$  before being detected, we change our strong measurement of  $P$  to one of  $K'$ , which is a combination of  $X$  and  $P$  [32] (see Supplemental Material [23]). Then we make a joint weak-strong measurement of  $X$  and  $K'$  in exactly the same manner as we did for the Dirac distribution to experimentally measure  $\tilde{\mathbb{P}}(x, k')$ . We repeat the experiment [Fig. 4(a)] and theoretical [Fig. 4(b)] Bayes' propagation (see the Supplemental Material [23]) for three values of  $\Delta z$  and plot the results in Figs. 4(i)–4(iii).

As  $\Delta z$  is increased, the distributions in Fig. 4 exhibit a broadening of  $\tilde{\mathbb{P}}(x, k')$  in the  $K'$  direction. This is due to the broad width of the photon state in  $X$  and the fact that the  $X$  portion of the hybrid  $X, P$  variable  $K'$  increases as  $\Delta z$  is increased. Also apparent is a growing  $k'$  displacement of the  $x > 25$  mm portion of the state as  $\Delta z$  is increased. This is consistent with a wedge in our oscillating glass plate of 0.4 arcseconds. Evidently, each of the three pairs of experimental and theoretical distributions agrees well in a qualitative manner, which confirms the applicability of classical-like Bayesian propagation.

In conclusion, by experimentally measuring the Dirac quasiprobability distribution we have completely determined a mixed quantum state. We have also demonstrated that the Dirac distributions measured at different spatial planes are related by Bayes' law, which therefore acts as a propagator of the quasiprobability. Quasiprobability distributions such as the  $Q$ ,  $P$ , or Wigner function reflect the arbitrary choice of the operator ordering (normal, anti-normal, or symmetric) that embodies the inherent incompatibility of quantum and classical physics. Missing from this list has been the standard ordering, the Dirac quasiprobability distribution, which has three outstanding features: (1) Its measurement is simple and similar to the classical equivalent. (2) It is compatible with Bayes' theorem, with which we can propagate it to other points in space or time. (3) In the limit of a pure quantum state, it reduces to quantum wave function itself.

We thank A. M. Steinberg and H. F. Hofmann.

\*charles.bamber@nrc-cnrc.gc.ca

†jlundeen@uottawa.ca

- [1] E. P. Wigner, *Phys. Rev.* **40**, 749 (1932).
- [2] R. Hudson, *Rep. Math. Phys.* **6**, 249 (1974).
- [3] N. Harrigan and R. Spekkens, *Found. Phys.* **40**, 125 (2010); R. Colbeck and R. Renner, *Nat. Commun.* **2**, 411 (2011); M. F. Pusey, J. Barrett, and T. Rudolph, *Nat. Phys.* **8**, 476 (2012); R. Colbeck and R. Renner, *Phys. Rev. Lett.* **108**, 150402 (2012); P. G. Lewis, D. Jennings, J. Barrett, and T. Rudolph, *Phys. Rev. Lett.* **109**, 150404 (2012).
- [4] K. Banaszek and K. Wódkiewicz, *Phys. Rev. Lett.* **82**, 2009 (1999); G. Brida, M. Genovese, M. Gramegna, C. Novero, and E. Predazzi, *Phys. Lett. A* **299**, 121 (2002); C. Ferrie and J. Emerson, *J. Phys. A* **41**, 352001 (2008); R. W. Spekkens, *Phys. Rev. Lett.* **101**, 020401 (2008); W. Son, J. Kofler, M. S. Kim, V. Vedral, and C. Brukner, *ibid.* **102**, 110404 (2009); J. J. Wallman and S. D. Bartlett, *Phys. Rev. A* **85**, 062121 (2012).
- [5] A. Mari and J. Eisert, *Phys. Rev. Lett.* **109**, 230503 (2012); V. Veitch, C. Ferrie, D. Gross, and J. Emerson, *New J. Phys.* **14**, 113011 (2012).
- [6] H. J. Groenewold, *Physica (Amsterdam)* **12**, 405 (1946).
- [7] G. S. Agarwal and E. Wolf, *Phys. Rev. D* **2**, 2161 (1970).
- [8] G. S. Agarwal and E. Wolf, *Phys. Rev. D* **2**, 2187 (1970).
- [9] A. Royer, *Phys. Rev. A* **15**, 449 (1977).
- [10] K. Husimi, *Proc. Phys. Math. Soc. Jpn.* **22**, 264 (1940).
- [11] R. J. Glauber, *Phys. Rev.* **131**, 2766 (1963); E. C. G. Sudarshan, *Phys. Rev. Lett.* **10**, 277 (1963).
- [12] K. Vogel and H. Risken, *Phys. Rev. A* **40**, 2847 (1989); K. Banaszek and K. Wódkiewicz, *Phys. Rev. Lett.* **76**, 4344 (1996); U. Leonhardt, *Measuring the Quantum State of Light*, *Cambridge Studies in Modern Optics* (Cambridge University Press, Cambridge, England, 1997); L. G. Lutterbach and L. Davidovich, *Phys. Rev. Lett.* **78**, 2547 (1997); P. Bertet, A. Auffeves, P. Maioli, S. Osnaghi, T. Meunier, M. Brune, J. M. Raimond, and S. Haroche, *ibid.* **89**, 200402 (2002); J. F. Kanem, S. Maneshi, S. H. Myrskog, and A. M. Steinberg, *J. Opt. B* **7**, S705 (2005); M. Hofheinz, H. Wang, M. Ansmann, R. C. Bialczak, E. Lucero, M. Neeley, A. D. O'Connell, D. Sank, J. Wenner, J. M. Martinis, and A. N. Cleland, *Nature (London)* **459**, 546 (2009); K. Laiho, K. N. Cassemiro, D. Gross, and C. Silberhorn, *Phys. Rev. Lett.* **105**, 253603 (2010).
- [13] E. Mukamel, K. Banaszek, I. A. Walmsley, and C. Dorrer, *Opt. Lett.* **28**, 1317 (2003); B. J. Smith, B. Killett, M. G. Raymer, I. A. Walmsley, and K. Banaszek, *ibid.* **30**, 3365 (2005).
- [14] P. A. M. Dirac, *Rev. Mod. Phys.* **17**, 195 (1945).
- [15] N. H. McCoy, *Proc. Natl. Acad. Sci. U.S.A.* **18**, 674 (1932).
- [16] J. G. Kirkwood, *Phys. Rev.* **44**, 31 (1933); Y. P. Terletsky, *Zh. Eksp. Teor. Fiz.* **7**, 1290 (1937); D. C. Rivier, *Phys. Rev.* **83**, 862 (1951); A. O. Barut, *ibid.* **108**, 565 (1957); H. Margenau and R. N. Hill, *Prog. Theor. Phys.* **26**, 722 (1961); M. Levin, *IEEE Trans. Inf. Theory* **10**, 95 (1964); A. Rihaczek, *ibid.* **14**, 369 (1968); M. Ackroyd, *Radio Electron. Eng.* **39**, 145 (1970).
- [17] L. Praxmeyer and K. Wódkiewicz, *Opt. Commun.* **223**, 349 (2003).
- [18] S. Chaturvedi, E. Ercolessi, G. Marmo, G. Morandi, N. Mukunda, and R. Simon, *J. Phys. A* **39**, 1405 (2006).
- [19] G. J. Pryde, J. L. O'Brien, A. G. White, T. C. Ralph, and H. M. Wiseman, *Phys. Rev. Lett.* **94**, 220405 (2005); K. J. Resch, J. S. Lundeen, and A. M. Steinberg, *Phys. Lett. A* **324**, 125 (2004); R. Mir, J. S. Lundeen, M. W. Mitchell, A. M. Steinberg, J. L. Garretson, and H. M. Wiseman, *New J. Phys.* **9**, 287 (2007); N. S. Williams and A. N. Jordan, *Phys. Rev. Lett.* **100**, 026804 (2008); O. Hosten and P. Kwiat, *Science* **319**, 787 (2008); J. S. Lundeen and A. M. Steinberg, *Phys. Rev. Lett.* **102**, 020404 (2009); K. Yokota, T. Yamamoto, M. Koashi, and N. Imoto, *New J. Phys.* **11**,

- 033011 (2009); P. B. Dixon, D. J. Starling, A. N. Jordan, and J. C. Howell, *Phys. Rev. Lett.* **102**, 173601 (2009); A. Feizpour, X. Xing, and A. M. Steinberg, *ibid.* **107**, 133603 (2011); S. Kocsis, B. Braverman, S. Ravets, M. J. Stevens, R. P. Mirin, L. K. Shalm, and A. M. Steinberg, *Science* **332**, 1170 (2011).
- [20] Y. Aharonov, D. Z. Albert, and L. Vaidman, *Phys. Rev. Lett.* **60**, 1351 (1988).
- [21] J. S. Lundeen and C. Bamber, *Phys. Rev. Lett.* **108**, 070402 (2012).
- [22] E. Arthurs and J. Kelly, *Bell Syst. Tech. J.* **44**, 725 (1965); L. M. Johansen and P. A. Mello, *Phys. Lett. A* **372**, 5760 (2008); A. Kalev and P. A. Mello, *J. Phys. A* **45**, 235301 (2012); A. Di Lorenzo, *Phys. Rev. Lett.* **110**, 010404 (2013); S. Wu, *Sci. Rep.* **3**, 1193 (2013).
- [23] See the Supplemental Material at <http://link.aps.org/supplemental/10.1103/PhysRevLett.112.070405> for additional technical detail and conceptual background information.
- [24] R. Jozsa, *Phys. Rev. A* **76**, 044103 (2007).
- [25] A. M. Steinberg, *Phys. Rev. A* **52**, 32 (1995).
- [26] H. F. Hofmann, *New J. Phys.* **14**, 043031 (2012).
- [27] J. S. Lundeen, B. Sutherland, A. Patel, C. Stewart, and C. Bamber, *Nature (London)* **474**, 188 (2011).
- [28] J. Z. Salvail, M. Agnew, A. S. Johnson, E. Bolduc, J. Leach, and R. W. Boyd, *Nat. Photonics* **7**, 316 (2013).
- [29] J. S. Lundeen and K. J. Resch, *Phys. Lett. A* **334**, 337 (2005).
- [30] H. F. Hofmann, [arXiv:1306.2993](https://arxiv.org/abs/1306.2993); T. Morita, T. Sasaki, and I. Tsutsui, *Prog. Theor. Exp. Phys.* (2013) 053A02.
- [31] S. M. Barnett, D. T. Pegg, and J. Jeffers, *J. Mod. Opt.* **47**, 1779 (2000); C. M. Caves, C. A. Fuchs, and R. Schack, *Phys. Rev. A* **65**, 022305 (2002).
- [32] A. W. Lohmann, *J. Opt. Soc. Am. A* **10**, 2181 (1993).